Chemical Engineering Science 117 (2014) 455–464

Contents lists available at ScienceDirect

Chemical Engineering Science

journal homepage: www.elsevier.com/locate/ces

Identify of flow patterns in bubbling fluidization

Yunning Li [a], Hui Fan [b], Xianfeng Fan [a,*]

[a] Institute for Materials and Processes, School of Engineering, The University of Edinburgh, Edinburgh EH9 3JL, UK
[b] College of Medical and Dental Sciences, The University of Birmingham, Birmingham B15 2TT, UK

HIGHLIGHTS

- Experiments conducted in a 3D gas/solid fluidized bed via the PEPT technique.
- Four flow structures within the bubbling regime.
- Flow Pattern Parameter has been developed.
- Flow Pattern Parameter can control and predict the fluidization performance.

GRAPHICAL ABSTRACT

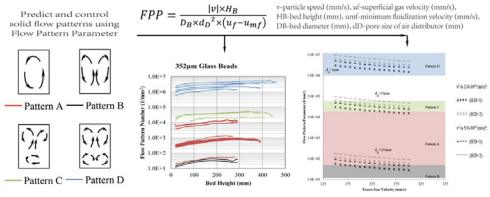

ARTICLE INFO

Article history:
Received 3 April 2014
Received in revised form
4 July 2014
Accepted 10 July 2014
Available online 17 July 2014

Keywords:
Bubbling fluidization
Flow structure
Air distributor
Superficial gas velocity
Solid properties

ABSTRACT

Bubbling fluidization has been widely applied in process industries, such as power generation from coal, renewable energy production, gasification and pyrolysis. In this study, we attempted to predict solid flow patterns in a bubbling fluidized bed based on operational conditions, the air distributor and particle velocity. We first investigated the effect of operational conditions and the air distributor on solid/gas flow patterns, and investigate the correlations between solid/gas flow patterns with the solid mixing, solid and gas contact, and bubble behaviour within bubbling fluidized beds by using positron emission particle tracking (PEPT). A 'Flow Pattern Parameter (FPP)' is then proposed to identify the solid flow pattern in a bubbling fluidized bed. The 'Flow Pattern Parameter (FPP)' consists of particle kinetic energy, bed aspect ratio (H/D), pore size of air distributor, minimum fluidization velocity, and superficial gas velocity. The results show that solid flow patterns in the bubbling fluidized bed can be clearly classified based on the Flow Pattern Parameter. Different flow pattern corresponds to a certain range of the Flow Pattern Parameter.

1. Introduction

Bubbling fluidization has been employed to many industrial processes, such as coal combustion and gasification, renewable energy production, chemical, petrochemical and metallurgical processes, granulation and drying (Di Maio et al., 2013; Salman and Hounslow, 2007). It has been demonstrated that the reaction efficiency, heat transfer and energy consumption in bubbling fluidization depend on solid mixing, solid–gas contact (Clift and Seville, 1993; He et al., 2004; Shibata et al., 1991), while solid mixing and solid and gas contact further depend on solid/gas flow structure or solid/gas flow pattern. Intensive research has been conducted to investigate the fluidization behaviour experimentally and numerically (Cloete et al., 2013; Gómez-Barea and Leckner, 2010; Herzog et al., 2012; Salman and Hounslow, 2007; Shi et al., 2011; Wardag and Larachi, 2012; Xiong et al., 2011), and many models have been developed for optimizing reactor design and bed scale up, and for identifying the effect of operational conditions, particle properties and bed design on fluidization behaviour. For example, Li et al. proposed an energy minimization multi-scale model (EMMS) to characterize the meso-scale structure of fluidization (Shi et al., 2011). Xiong et al. proposed a smoothed particle

* Corresponding author. Tel.: +44 1316505678.
E-mail address: x.fan@ed.ac.uk (X. Fan).

http://dx.doi.org/10.1016/j.ces.2014.07.012
0009-2509/

hydrodynamics method to solve problems in modelling dense particle-fluid fluidization (Xiong et al., 2011). Herzog et al. used different CFD-codes to predict pressure drop and bed expansion ratio in a gas-solid fluidized bed by considering solid-phase properties, momentum exchange coefficients (Herzog et al., 2012). Ku et al. used an Eulerian–Lagrangian approach to simulate a bubbling fluidized bed and analysed solid flow pattern, bed expansion, pressure drop and fluctuation by considering drag force correlations, particle-particle and particle-wall collisions (Ku et al., 2013). Wang et al. developed a drag model to simulate the meso-scale structure in solid–gas bubbling fluidized beds. Their simulated results have a good agreement with experimental data (Wang et al., 2013). Olsson et al. experimentally investigated the fuel dispersion in a large scale bubbling fluidized bed with a cross section area of 1.44 m^2 through analysing the effect of operational conditions and fuel particle properties on the local mixing mechanisms and lateral fuel dispersion (Olsson et al., 2012). Fotovat et al. investigated the gas distribution in a bubbling fluidized bed and the effect of solid loading and biomass quantity on bubble void fraction and distribution (Fotovat et al., 2013). Vakhshouri and Grace found that fluidization models have always neglected the effect of plenum chamber volume on fluidization behaviour and experimentally investigated its effect on the behaviour of FCC and glass particle bed (Vakhshouri and Grace, 2010).

However many factors can affect solid/gas flow pattern in a fluidized bed and make fundamental analysis, modelling and prediction of fluidization behaviour difficult and in some cases impossible. In a fluidized bed, gas flow is introduced into a bed through a gas distributor and forms many bubbles or voids. The bubbles or voids drive solid particles circulating around within the bed (Garcia-Gutierrez et al., 2013; Laverman et al., 2012; Soria-Verdugo et al., 2011). The circulation pattern is determined by the bubble size, bubble rise velocity, and bubble distribution within the bed, which further depend on superficial gas velocity, pore size of air distributor, density and size of solid particles, column diameter etc. All of these factors are interrelated, but we do not know their relative importance (Ding et al., 2006). For example, bubbles drive particles, and the moving particles interact with bed wall and packed particles, in turn the interaction between particles and bubbles affect the macroscopic and microscopic behaviour of the bed, bubble size, bubble rise velocity, and bubble distribution (Ding et al., 2006; Smoulders and Baeyens, 2001; Wang et al., 2011).

Several experimental techniques have also been developed to measure and analyse the fluidization behaviour and the effect of various factors, such as positron emission particle tracking technique (PEPT) (Laverman et al., 2012; Parker et al., 1997, 1993), X-ray densitometry/tomography (Saayman et al., 2013), electrical capacitance volume tomography (Weber and Mei, 2013), ultra-fast magnetic resonance imaging, the measurement of pressure fluctuations (Sedighikamal and Zarghami, 2013), LDV measurement and analysis of gas and particulate phase velocity profiles (Mychkovsky and Ceccio, 2012), laser Doppler anemometry (LDA), cross-sectional wire mess sensors.

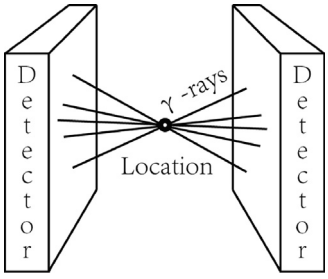

Fig. 1. Schematic diagram of PEPT.

In this study, we use PEPT to directly measure the impact of the operation parameters and air distributor on solid and gas behaviour in a bubbling fluidized bed. We will investigate the effect of aspect ratio (H/D), pore size of air distributor, and superficial gas velocity on fluidization, and then provide a form of equation to identify the flow structure in bubbling fluidization regime based on bed design and operational conditions.

2. Positron emission particle tracking (PEPT) technique

The positron emission particle tracking (PEPT) has been developed to track lubricant flow in aircraft engines at the University of Birmingham in 1980'. Recent development has extended its application to track 1–3 particles in opaque vessels or dense systems accurately and non-invasively, to study multiphase flow, such as granular materials and viscous fluid flows, in engineering processes. The technique employed 1–3 radioactively labelled particles and a pair of positron-sensitive γ-ray detectors to receive the γ-rays emitting from tracer particles. An iterative algorithm has also been developed to calculate the tracer positions (Yang et al., 2007a, 2007b). The tracer particles are normally labelled by ^{18}F, ^{61}Cu or ^{66}Ga. These radioisotopes decay via β^+ decay and emit positrons. The positron rapidly annihilates with an electron and gives γ-rays. In PEPT technique, we are interested in the γ-rays with energy of 511 keV because they emit in pair and as counter-propagating γ-rays. Theoretically, all the counterpropagating γ-rays should meet at a point in space where the tracer particle is located (Fig. 1). The two detectors designed to capture γ-ray pairs simultaneously and the tracer locations can be defined from the collected γ-ray pairs. In practice, many γ-rays are corrupted, and lines connecting the two ends of counterpropagating γ-rays which are detected by the two detectors do not pass the tracer source. Therefore, the location algorithm (Yang et al., 2007a, 2007b) has been developed to discard the corrupted γ-ray events and calculate the actual tracer position.

The location algorithm starts from calculating the distances of a point perpendicular to the all gamma ray trajectories, and then finds the point that minimizes the sum of the distances (Yang et al., 2007a, 2007b). For example, for a giving set of γ-ray M, the sequential trajectories named as $M_1 \ldots M_N$, the summation of distances from point (x,y,z) to all γ-ray trajectories is

$$D_M(x,y,z) = \sum_s d_i(x,y,z)\ (\text{mm}) \tag{1}$$

The minimum solution for the sum of distance is then obtained from

$$\begin{cases} \frac{\partial D_M(x,y,z)}{\partial x} = 0 \\ \frac{\partial D_M(x,y,z)}{\partial y} = 0 \\ \frac{\partial D_M(x,y,z)}{\partial z} = 0 \end{cases} \tag{2}$$

The first approximation of the minimum distance from the point (x_0,y_0,z_0) can be calculated based on Eq. (2) with a mean deviation of

$$\delta_M(x_0,y_0,z_0) = \frac{D_M(x_0,y_0,z_0)}{N(M)}\ (\text{mm}) \tag{3}$$

where $\delta_i(x,y,z)$ is the distance between point (x,y,z) and the ith trajectory; $N(M)$ is the events number in the set M.

The distance of the point (x_0,y_0,z_0) to all trajectories within the set M are calculated and each trajectory with a distance$d_i(x_0,y_0,z_0)$ larger than $k\delta_s(x_0,y_0,z_0)$ is discarded, here k is a constant. After discarding the corrupt events, more accurate tracer location (x_1,y_1,z_1)can be calculated using the subset events M_1 with a renewed mean difference of $\delta_{s1}(x_1,y_1,z_1)$. Following the same iteration principle process, and discarding the corrupted events